JOURNAL OF GUIDANCE, CONTROL, AND DYNAMICS
Vol. 29, No. 1, January–February 2006

# Tractable Conflict Risk Accumulation in Quadratic Space for Autonomous Vehicles

Thomas Jones*
*University of Stellenbosch, Stellenbosch 7602, South Africa*

**Recent developments have shown that conflict avoidance may be cast as a probabilistic state-space problem. The probabilistic accumulation of risk because of exposure to a hazard over a period of time is an essential and often neglected and misunderstood aspect of the process of conflict risk calculation. How such risk accumulation may be accurately approximated in real time is demonstrated. The research reverts to theoretical basics and illustrates how risk accumulation for a one- and two-vehicle scenario is a first passage time problem. It is illustrated how exact quadratic state-order reduction may be combined with simple and accurate first passage time approximations. In this way, a tractable and accurate receding horizon solution is provided with the recognition of the time dependence of risk accumulation. The solution algorithm is implemented as a relatively straight-forward four-step discrete-time propagation and accumulation of risk. Small calculation errors are characterized to first order–second moment and always lead to a slight upper-bound solution, thereby improving safety. Simulation results indicate a high degree of risk calculation accuracy, calculable in real time.**

## Nomenclature

| | | |
|---|---|---|
| $D_f$, $D_s$ | = | domains of failure and safety respectively |
| $E[a]$ | = | expected value of random variable $a$ |
| $f_X(x)$ | = | probability density function (PDF) of $x$ |
| $f_{X(k)}(x)\|B[a, k-1]$ | = | PDF of $x$ at time $t_k$, conflict free within $[t_a, t_{k-1}]$ |
| $f_{X(k)}^{B(k)}(x)$ | = | PDF of $f_{X(k)}(x)\|B[0, k-1]$ with $x \in D_f$ segment removed |
| $g_{A(k)}(x)$, $g_{B(k)}(x)$ | = | segments of $f_{X(k)}(x)\|B[0, k-1]$, where $x \in D_f$ and $x \notin D_f$, repectively |
| $K$ | = | number of discrete-time steps |
| $N(m, \Sigma)$ | = | normal distribution with mean $m$ and covariance $\Sigma$ |
| $P_c(k) \equiv P_c(t_k)$ | = | total probability of conflict accumulated over the interval $[t_0, t_k]$ |
| $\gamma$ | = | quadratic conflict metric |
| $\bar{\gamma}$ | = | conflict threshold |
| $\Delta E[a]$ | = | change in expected value of $a$ |
| $\Delta t$ | = | time step size |
| $\Delta\gamma$, $\Delta\dot{\gamma}$, $\Delta\Gamma$, $\Delta\dot{\Gamma}$ | = | short for $\Delta t\gamma$, $\Delta t\dot{\gamma}$, $\Delta t\Gamma$, and $\Delta t\dot{\Gamma}$, respectively |
| $\delta(t)$ | = | Dirac delta function |
| $\phi_\Gamma(\tau)$ | = | characteristic function of $\gamma$ |
| $\nabla a$ | = | first-order–second-moment error in calculation of $a$ |

## I. Introduction

MOST uncrewed aerial vehicles (UAVs) and especially autonomous UAVs are required to avoid commercial airspace, unless the Federal Aviation Administration deems their detect and avoid capabilities to be on par with piloted systems. Automated conflict avoidance would assist in opening this door to commercial airspace, especially for autonomous UAVs. This research builds toward the creation of automated conflict avoidance and air traffic management systems that could play the role of not only an alerting system, but also would automatically resolve intervehicle conflict on par with piloted commercial aviation systems.[1,2] As a natural first step, this paper focuses on conflict risk calculation.

Human operators add the complexity of unknown pilot intent to the conflict avoidance equation. Conflict avoidance, by definition, includes the capability to propagate vehicle state to predict future intervehicle conflict. As such, uncertainty of pilot intent hampers the accuracy of conflict detection.[2] Most autopilots are deterministic, and models of their operation may be created with an accuracy far exceeding that of human operator models. As such, autonomous UAVs provide a unique opportunity for the creation of more accurate and reliable conflict detection systems.

Last, there is a connection between the performance of a conflict avoidance system and the occurrence of false alarms.[3] False alarms lead to mistrust, thereby reducing a system's effectiveness, in accordance with such principles as risk homogenization and negative reinforcement.[4] Pilots tend to be less inclined to take action after issuance of false alerts, thereby increasing the risk of conflict during a valid alert. Autonomous UAVs do not suffer from the same adverse consequences, and false alarms are, therefore, less problematic.

Kuchar[3] showed that conflict alerting systems are but a part of several safety components in complex vehicle systems, as shown in Fig. 1.

Together, the environment, conflict detection, and conflict resolution form a conflict avoidance system. For autonomous vehicles, such a system monitors the environment, predicts vehicle-relative state, issues alerts, and plans and executes avoidance trajectories (conflict resolution). This is different from traditional conflict avoidance systems in which alerts are issued, but resolution is accomplished by a human.

Ownship and air traffic state must be monitored. As with most alerting systems, it is assumed that the estimated state variables are of a multivariate normal distribution.[5,6] Trajectory intent is established using models of the autopilot and trajectory planning systems of vehicles and also knowledge of flight plans and waypoints. A closed-loop dynamic model of the vehicle must be known, and when combined with pilot intent, one may propagate current state estimates.

Alerting parameter(s), also known as conflict metrics, are employed to judge whether conflicts are likely. Probabilistic systems typically calculate a probability of conflict, that is, a probability of exceeding the safety thresholds of a conflict metric. The conflict avoidance system may demand action when certain risk probability thresholds are exceeded. Part of the focus of this paper is on defining a conflict metric in such a way as to reduce the state order, and thus complexity, of the conflict avoidance problem.

Received 30 April 2004; revision received 30 March 2005; accepted for publication 1 April 2005. 

*Senior Lecturer, Department of Electrical and Electronic Engineering, Private Bag X1, Matieland. Member AIAA.

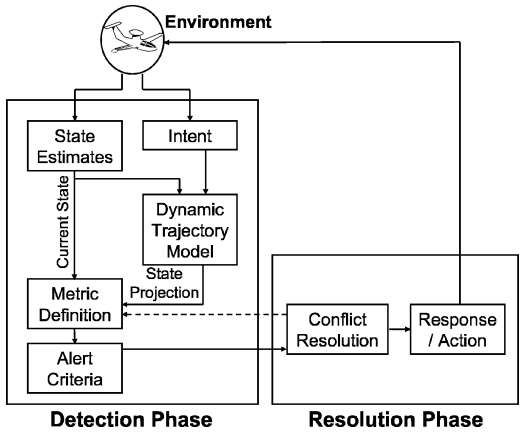


**Fig. 1 Block diagram of the Conflict detection and resolution process.**

### A. State-Space Representation

Kuchar[3,7] defines the time-dependent state vector

$$x(t) = [x_1(t), \ldots, x_n(t)]^T \tag{1}$$

where $n$ is the system order, each state variable $x_i(t)$ represents a parameter that may in some way be employed by the alerting logic, and $x(t) \in \boldsymbol{R}^n$.

In general, there are regions of, or subsets in, the state space $\boldsymbol{R}^n$ that are hazardous to the vehicle. In this development such a region is referred to as a domain of failure, denoted by $D_f(t) \subset \boldsymbol{R}^n$, in accordance with reliability theory.[8]

The dynamics, state, and relevant avoidance trajectories of a vehicle require that an alert be issued reasonably far outside of $D_f(t)$ to ensure that a conflict does not occur. This space is defined as the alert space $D_a(t)$, where $D_f(t) \subset D_a(t)$.

### B. Methods of Approach

Traditionally, conflict avoidance is solved through prediction of conflict events by means of single-path and worst-case approaches. Cited examples of these approaches are primarily taken from a survey paper by Kuchar and Yang.[1]

The single-path approach assumes that a vehicle follows a fixed trajectory, often a straight line, and that conflict occurs when a safety buffer around one vehicle is projected to intersect with $D_f(t)$. This is a deterministic approach with a definite hit or miss result.[9,10]

The worst-case approach propagates a vehicle's state trajectory according to its maximum dynamic capabilities. An alert is issued when it is predicted that $x(t) \in D_f(t)$ will occur within a time frame of interest. It is most useful for short durations of conflict prediction because trajectory deviations may be severe when projected at maximal rates.[11–13]

Most single-path and worst-case approaches may be implemented in real time because this is partly the purpose of their creation. These are tractable, approximate, deterministic solutions to a generally intractable probabilistic problem. Such methods do, however, suffer from inaccuracies brought on by approximation that manifest themselves as suboptimal false alarm and missed detection rates. Most of these systems are applicable to very specialized conflict avoidance problems and are highly sensitive to a vehicle's control strategy and dynamic model.[1,5]

The true probabilistic approach, as employed here, forms a middle ground between single-path and worst-case methods, but is usually avoided because of its computational intractability and because ad-hoc approximate solutions are usually created.[12,14] In this case, likelihood of conflict, defined as the likelihood of $x(t) \in D_f(t)$, is calculated within a given time horizon. Yang[5] views this as weighing all possible trajectories with their probability of occurrence and then summing the contributions of those crossing into $D_f(t)$. The probability of conflict accumulated over the interval $[t_0, t]$, as a function of time, will be denoted by $P_c(t)$. In this way, the amount of conflict risk accumulated from the start to the end of the time horizon, that is, within the interval $t = [t_0, t_h]$, becomes $P_c(t_h)$.

Probabilistic approaches may be solved through various techniques. In this paper, the creation of a tractable, deterministic algorithm is detailed. Monte Carlo simulation may also be employed, with apt approximations, as most recently documented by Yang et al.[15]

### C. First Passage Time Problem

The first passage time (FPT) problem is used to describe particle motion in physics.[16] Physicists are interested in understanding the motion of a molecule under the influence of uncorrelated interparticle collisions. The collisions are usually modeled as transfer of momentum from a Wiener excitation process, and the major interest, as applied to a single dimension of a homogeneous process, is to determine the probability of a particle exiting a displacement interval $(a, b)$, that is, of $x$ exiting $a \leq x \leq b$, where $a$ and $b$ are absorbing bounds. An absorbing bound is similar to the boundary of $D_f$ because entry into this domain (collision/conflict) is considered to be a failure and negates the possibility of exit from the domain.

This system described by an Ito stochastic differential equation of the form

$$\mathrm{d}x(t) = A[x(t), t]\,\mathrm{d}t + \sqrt{B[x(t), t]}\,\mathrm{d}W(t) \tag{2}$$

where $W(t)$ is a Wiener process.

Solving for the probability of leaving the interval as a function of time is then similar to solving for the probability of an aircraft entering into $D_f$, denoted by $P_c(t)$. This is especially evident when one bound, for example, $b$, is considered to be distant and the particle's initial position is much closer to $a$. $P_c(t)$ can then be solved through application of the backward Fokker–Planck (Kolmogorov) equation (see Ref. 17). This solution, even in one dimension, is of excessive complexity. Desilles[6] provides an example of how this process may be applied to the two-vehicle conflict avoidance problem.

An interesting aspect of the FPT representation is that it likens the calculation of conflict risk to the flow of probability space across a boundary, into a domain of failure, $D_f$. The risk calculation strategy presented here is developed from the standpoint of reliability theory, resulting in a solution that accumulates the amount of probability flow into $D_f(t)$ over time, thus providing an approximate solution to this FPT problem formulation.

## II. Tractable Discrete-Time FPT Problem Solution

FPT calculation complexity stems from the dimensionality of the risk accumulation problem, state-time correlation, and especially the conditionality of state distribution on conflict events. It is shown how to perform the required calculations and then how to make the calculations tractable is described, thereby avoiding the need for, for example, Monte Carlo probes of the probability space. This research is constrained to dealing with a single-vehicle–single-obstacle problem. Two-vehicle problems may be transformed into a single-vehicle relative frame, thereby reducing it to a single-vehicle–single-obstacle problem.[18]

### A. Accumulation of Risk

The accumulation of risk over time is explained with the help of the discrete representations in Figs. 2 and 3. Figure 2 illustrates the basic FPT concept of risk accumulation. The state distribution is propagated forward at discrete-time intervals because analytical solutions to this procedure do not exist. After every time step, the intersection between the distribution and the hazard (domain of failure) is integrated to provide the added risk accumulated over that time step. The section intersecting with the hazard is cut from the distribution, and the remaining distribution is propagated to the next time step, and so forth.

Two interesting aspects of risk accumulation should be noted.

1) The problem may be described as a flow of probability space into a hazard, over a short-time interval. It is this probability density flow into the hazard that undergoes volumetric integration at each time step and is then summed over a finite horizon.

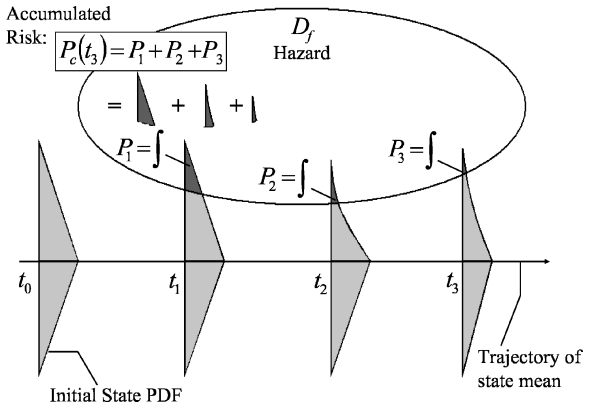


**Fig. 2 Basic two-dimensional risk accumulation, with one-dimensional initial state distribution.**

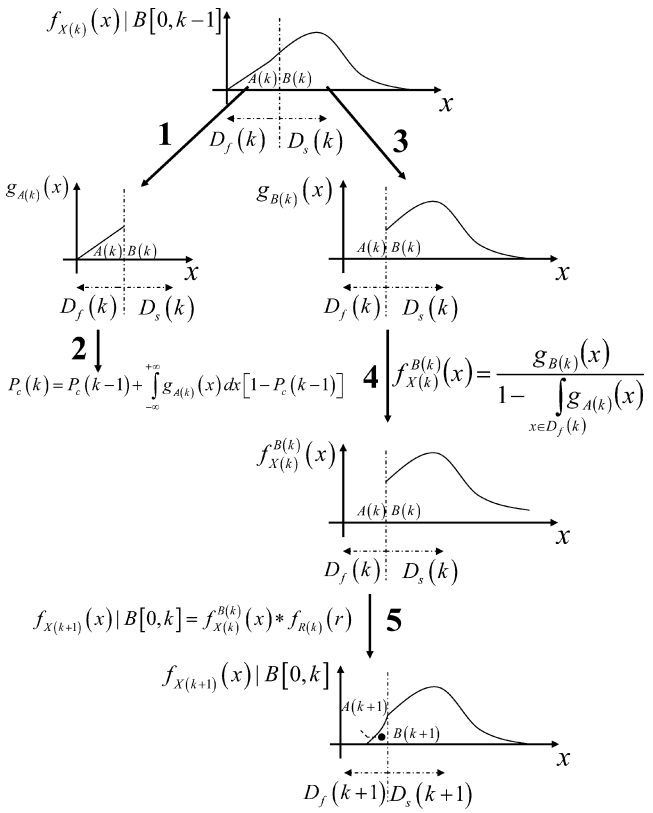


**Fig. 3 Five-step $f_{X(k+1)}(x)|B[0,k]$ propagation and calculation of $P_c(k)$ (one dimensional).**

2) The hazard absorbs the probability space because space that has already collided (conflicted) with the hazard should not be propagated any further. One way to understand the absorption (refer to the FPT problem) is to view the state probability density as a cloud of possible vehicles and to recognize that a vehicle entering the hazard should be removed from further calculations because it has already conflicted. This results in a conditional-state distribution at every time interval, and the implications are that the probability space diminishes as time progresses, conflict risk increases with time exposure to the hazard, and state distribution no longer remains Gaussian.

The aim is to describe conflict risk accumulated within the discretized interval $t=[t_0, t_{K-1}]$, where $t_{K-1}\equiv t_h$ is the finite horizon time and $t=t_0$ is considered to be the present, that is, the point in time when one needs to determine conflict risk within the next $t_w=t_{K-1}-t_0$ seconds. Now write the conflict probability similarly to the FPT probability, that is, the probability of entering the domain of failure by the time $t=t_k$, as

$$\begin{aligned}P_c(k)&=P[x(t)\in D_f(t),\text{ exactly once in }[t_0,t_k]],\qquad \forall k>0\\&=P[x(0)\in D_f(0)]\\&\quad+\sum_{i=1}^{k}\left\{P\left[x(i)\in D_f(i)\,|\bigcap_{j=0}^{i-1}x(j)\notin D_f(j)\right][1-P_c(i-1)]\right\}\\&=P\left[x(k)\in D_f(k)\,|\bigcap_{j=0}^{k-1}x(j)\notin D_f(j)\right]P_c(k-1),\qquad \forall k>0\end{aligned}\tag{3}$$

where $k\equiv t_k$ to shorten the discrete notation. For the continuous time case, $K\to\infty$ and, therefore, $\Delta t\to 0$. The continuous case is the multidimensional statement of the FPT problem. In Eq. (3), it is assumed that the vehicle has not conflicted before $t=t_0$.

Solving Eq. (3) in its given form is a complicated task. Equation (3) may be written in a different form, by recognizing that one may propagate the probability density function (PDF) of the state space remaining outside of $D_f(t_k)$ throughout $[t_0, t_k]$.

*Definition:* Here $f_{X(t_k)}(x)|B[0, k-1]$ is the time-variant PDF of the state $x(t)$ at the discrete time $t=t_k$, conditioned on the fact that no conflict has occurred while $t\in[t_0, t_{k-1}]$. The conditionality is denoted by $B[0, k-1]$.

At time $t=t_0$, the start of the propagation, and writing $k\equiv t_k$ for short, the conditional PDF is equivalent to the marginal PDF

$$f_{X(0)}(x)=g_{A(0)}(x)+g_{B(0)}(x)\tag{4}$$

where $g_{A(0)}(x)$ and $g_{B(0)}(x)$ are the segments of the PDF inside and outside of $D_f(0)$, respectively. At time $t=t_0+k.\Delta t$, $k$ discrete time steps later, the equation becomes

$$f_{X(k)}(x)|B[0,k-1]=g_{A(k)}(x)+g_{B(k)}(x)\tag{5}$$

Writing Eq. (3) in terms of Eqs. (4) and (5), one may express the accumulated probability of conflict up to the discrete time $t=t_k$ as

$$\begin{aligned}P_c(k+1)&=\int_{x\in D_f(0)} g_{A(0)}(x)\,\mathrm{d}x\\&\quad+\int_{x\in D_f(1)} g_{A(1)}(x)\,\mathrm{d}x[1-P_c(0)]+\cdots\\&\quad+\int_{x\in D_f(k)} g_{A(k)}(x)\,\mathrm{d}x[1-P_c(k-1)]\\&\quad+\int_{x\in D_f(k+1)} g_{A(k+1)}(x)\,\mathrm{d}x[1-P_c(k)]\\&=P_c(k)+\int_{x\in D_f(k+1)} g_{A(k+1)}(x)\,\mathrm{d}x[1-P_c(k)]\end{aligned}\tag{6}$$

In this way, it is clear that $P_c(k)$ may be determined through an incremental update at each time step from $t=t_{k-1}$ to $t=t_k$, with $P_c(k<0)=0$, provided that $g_{A(k)}(x)$ can be found for $0\le k\le(K-1)$. Finding $g_{A(k)}(x)$ entails expressing $f_{X(k)}(x)|B[0,k-1]$ and salvaging the segment of $f_{X(k)}(x)|B[0,k-1]$ inside $D_f(k)$, according to Eqs. (4) and (5). As such, one needs to focus on calculating $f_{X(k)}(x)|B[0,k-1]$.

At time $t=t_0$, one starts with the marginal PDF $f_{X(0)}(x)$, then needs to find $f_{X(1)}(x)|B[0,0]$, and so forth. In general, calculate $f_{X(k+1)}(x)|B[0,k]$ when $f_{X(k)}(x)|B[0,k-1]$ is known and $f_{X(0)}(x)|B[0,-1]=f_{X(0)}(x)$. To do this, one needs to understand

how $x(k+1)$ can be realized from $x(k)$. When application of discrete Euler integration (for simplicity) is assumed, now express

$$\begin{aligned} x(k+1) &= x(k) + \Delta t \dot{x}(k) \\ &= [I + \Delta t A(k)]x(k) + [\Delta t B(k)u(k) + \Delta t B(k)w(k)] \\ &= M_k[x(k)] + R_k[u(k), w(k)] \end{aligned} \tag{7}$$

where $M_k[x(k)]$ and $R_k[u(k), w(k)]$ are independent quantities. This independence allows us to apply $n$-dimensional convolution to find

$$f_{Xk+1}(x) = f_{Mk}(m) \times f_{Rk}(r) \tag{8}$$

In the same way, propagate $f_{X(k)}(x)|B[0, k-1]$ by setting

$$\begin{aligned} f_{X(k+1)}(x)|B[0,k] &= \frac{g_{B(k)}(x)}{\int_{x \notin D_f(k)} g_{B(k)}(x)} \times f_{Rk}(r) \\ &= \frac{g_{B(k)}(x)}{1 - \int_{x \in D_f(k)} g_{A(k)}(x)} \times f_{Rk}(r) \\ &= f^{B(k)}_{X(k)}(x) \times f_{Rk}(r) \end{aligned} \tag{9}$$

where

$$f^{B(k)}_{X(k)}(x) \equiv \frac{g_{B(k)}(x)}{1 - \int_{x \in D_f(k)} g_{A(k)}(x)} \tag{10}$$

and with $P_c(-1) = 0$. In Eq. (9), $g_{B(k)}(x)$ represents the segment of $f_{X(k)}(x)|B[0, k-1]$ outside of $D_f(k)$ and

$$\int_{x \notin D_f(k)} g_{B(k)}(x)$$

normalizes $g_{B(k)}(x)$ to become a true PDF, in accordance with Bayes rule. It is essential to realize that only that part of $f_{X(k)}(x)|B[0, k-1]$ outside of $D_f(k)$ must be propagated because $f_{X(k+1)}(x)|B[0, k]$ is by definition conditioned on $B[0, k]$. No closed-form representation of the convolution in Eq. (9) is, however, known, and the computational complexity of a numerical solution is $\mathcal{O}(N^{2n})$, with $N$ being the number of quantizations of each dimension of the space and $n = \dim(x)$.

### B. Propagation Procedure

Thus far, assumptions have been made about the nature of the system under consideration, such as linearity and time variance. This is also a one-vehicle–one-obstacle problem (equivalent to a two-vehicle problem[18]), with normally distributed states. Given these assumptions and accepting that the vehicle has not been in conflict before $t = t_0$ (or by defining the probability of conflict only within $[t_0, t_h]$), then the developments from Eqs. (3–9) are accurate discrete-time representations.

Figure 3 shows how the discrete-time probability of conflict accumulated within $[t_0, t_k]$, denoted by $P_c(k)$, may be found through a five-step propagation process. Figure 3 is provided for a one-dimensional problem to reinforce understanding of the process. Notice that the propagation process requires knowledge of $P_c(k-1)$ to find $P_c(k)$. This implies that the five-step process needs to be applied incrementally for each discrete-time step in $[t_0, t_k]$, starting at $t_0$. Recall the initial conditions: $f_{X(0)}(x)|B[0, -1] = f_{X(0)}(x)$ and $P_c(-1) = 0$, then at every time step $t = t_k$.

1) Segment $g_{A(k)}(x)$ from $f_{X(k)}(x)|B[0, k-1]$ by setting $f_{X(k)}(x)|B[0, k-1] = 0 \,\forall\, x \notin D_f(k)$.

2) Use

$$P_c(k) = P_c(k-1) + \int_{x \in D_f(k)} g_{A(k)}(x)\, \mathrm{d}x [1 - P_c(k-1)]$$

to accumulate the probability of conflict.

3) Segment $g_{B(k)}$ from $f_{X(k)}(x)|B[0, k-1]$ by setting $f_{X(k)}(x)|B[0, k-1] = 0 \,\forall x \in D_f(k)$.

4) Normalize $g_{B(k)}$ to create the PDF

$$f^{B(k)}_{X(k)}(x) \equiv \frac{g_{B(k)}(x)}{\left[1 - \int_{x \in D_f(k)} g_{A(k)}(x)\right]}$$

5) Propagate $f^{B(k)}_{X(k)}(x)$ to the next time step through the $n$-dimensional convolution $f_{X(k+1)}(x)|B[0, k] = f^{B(k)}_{X(k)}(x) \times f_{Rk}(r)$.

Now continue the process by utilizing $f_{X(k+1)}(x)|B[0, k]$ at time $t = t_{k+1}$ to obtain $g_{A(k)}(x)$ as in step 1, and so forth. The numerical complexity of the propagation phase is dominated by the $\mathcal{O}(N^{2n})$ convolution process indicated in step 5 and described by Eq. (9). This results in intractability for meaningful values of $n$ and $N$.

### C. Sources of Computational Complexity

The numerical complexity of the preceding propagation phase is dominated by the $\mathcal{O}(N^{2n})$ convolution process indicated in step 5 and described by Eq. (9). It also seems like the $n$-dimensional integration of Eq. (6) could potentially add additional $\mathcal{O}(N^n)$ complexity to the solution. Fortunately, this integral may be solved through a gradient search approach of $\mathcal{O}(nN)$.[8]

Resolving $f_{X(k)}(x)|B[0, k-1]$ into $g_{A(k)}(x)$ and $g_{B(k)}(x)$, segments within and without of $D_f(k)$, respectively, adds complexity. This is because only $f^{B(k)}_{X(k)}(x)$, derived from $g_{B(k)}(x)$ [see Eq. (9)], must be propagated forward in time and it is no longer a simple normal distribution. Hence, analytical solutions to Eqs. (6) and (8) are unknown.

### D. Simplifying Assumptions

Existing conflict avoidance systems such as the Traffic Alert and Collision Avoidance System (TCAS) define a so-called distance modifier (DMOD). This is a conflict safety bound (distance)[19] around an aircraft, which corresponds to a radius of conflict.

It is in the spirit of TCAS, its well-established track record, and its wide acceptance as a standard for comparison[3,5,19,20] that a similar safety bound or DMOD is chosen to surround a vehicle. It will be shown that this tried and tested bound may in fact be shaped into a useful order reductive metric. In addition, the research also generalizes the metric to ellipsoid shapes around the vehicle, by defining it as a quadratic function of the vehicle's state described by

$$R = \sqrt{x^T B x} \tag{11}$$

where $B$ is constrained to be a real, symmetric positive definite matrix.

The square of the $R$ metric is more useful because the square root operator in Eq. (11) spawns considerable numerical and analytical complexity when calculating PDFs. The metric, therefore, becomes

$$\gamma = R^2 = x^T B x \tag{12}$$

For typical spherical buffers around vehicles where position is a simple state, $B$ only retains sparse unitary diagonal entries.

### E. Mathematical Reduction

Now reduce the required convolution order of the $n$-dimensional state distribution by applying the one-dimensional metric. The conflict safety bound [the boundary of $D_f(t)$] of an aircraft must be expressed in the form of Eq. (12) to apply the algorithms developed herein.

Define $\bar{\gamma}$ as the conflict threshold (often the square of the DMOD) or the boundary of $D_f$, that is, if

$$\gamma \leq \bar{\gamma} \tag{13}$$

then conflict has occurred. Equation (13) now becomes the order reductive conflict metric of interest. The aim is to determine the probability of satisfying this inequality within $[t_0, t_k]$, which is equivalent

to evaluating the probability of conflict, $P_c(k)$. The full-state representation of Eq. (7) may be replaced by the single-state equivalent,

$$\gamma(k+1) = \gamma(k) + \Delta t\dot{\gamma}(k) = \gamma(k) + \Delta\dot{\gamma}(k) \tag{14}$$

where $\Delta t\dot{\gamma}(k)$ will be referred to as $\Delta\dot{\gamma}(k)$ to avoid complicated notation. In addition, it will be shown that $\Delta\dot{\gamma}(k)$ can also be conveniently expressed as a quadratic form of $x$.

Recognize, from elementary probability theory, that the cumulative distribution function of $\gamma(k+1)$ is described by $F^{B(k+1)}_{\Gamma(k+1)}(\gamma) \equiv P[\Gamma(k+1) < \gamma | B[0,k]$. In this way, the marginal PDF of $\gamma(k+1)$ may be described exactly by

$$f_{\Gamma(k+1)}(\gamma)|B[0,k] = \frac{\mathrm{d}}{\mathrm{d}\gamma}\int_{-\infty}^{+\infty}\int_{-\infty}^{\gamma-\psi} f^{B(k)}_{\Gamma(k),\Delta\dot{\Gamma}(k)}(\psi,\phi)\,\mathrm{d}\phi\,\mathrm{d}\psi \tag{15}$$

where

$$f^{B(k)}_{\Gamma(k),\Delta\dot{\Gamma}(k)}(\gamma,\Delta\dot{\gamma}) \equiv \frac{\mathrm{d}^2}{\mathrm{d}\gamma\,\mathrm{d}\Delta\dot{\gamma}} F^{B(k)}_{\Gamma(k),\Delta\dot{\Gamma}(k)}(\gamma,\Delta\dot{\gamma}) \tag{16}$$

is the joint PDF of $\gamma$ and $\Delta\dot{\gamma}$ at $t = t_k$, given that no conflict has occurred within $[t_0, t_k]$. Also, $\psi$ and $\phi$ are variables of integration.

### F. Simplifying Approximations

The reductive conflict metric results in Eqs. (14–16), which are usually simpler to manipulate than their $n$-dimensional counterparts. There are, however, two issues not to be avoided without approximation

1) The double integral of Eq. (15) needs to be approximated with computational complexity of $\mathcal{O}(N^4)$, unless $\gamma$ and $\Delta\dot{\gamma}$ are independent, in which case complexity of $\mathcal{O}[N\log(N)]$ results.

2) No analytical solution is known to the joint PDF in Eq. (16). Numerical approximation would be of $\mathcal{O}(N^{2n+2})$ complexity because one would need to revert back to the full-state representation and, for example, employ a Monte Carlo method.

Approximation will need to fulfill at least two primary requirements.

1) The calculation-order complexity of Eqs. (15) and (16) needs to be reduced significantly.

2) Approximation errors need to be characterized to a sensible extent. All sign-indefinite errors must be calculated and sign-definite errors must at least be clamped between upper and lower bounds, with an emphasis on the calculation of the upper bound. Upper bounds on, for example, $P_c$ estimates lead to a more conservative and usually safer alerting approach for autonomous vehicles.

It is clear that the major issue of complexity is the calculation of Eq. (16). Recall that Eq. (3) provides the discrete representation of $P_c(k) \equiv P_c(t_k)$. The aim is to perform an accurate upper-bounded calculation that would provide an equivalent expression to Eq. (16), but of considerably reduced complexity. To this effect, and in accordance with other FPT application texts,[21–23] approximate

$$\begin{aligned}
P_c(k) &= P[x(t)\in D_f(t), \text{exactly once in } [t_0,t_k]], \qquad \forall k>0\\
&= P[x(0)\in D_f(0)]\\
&\quad + \sum_{i=1}^{k}\left\{P\left[x(i)\in D_f(i)\middle|\bigcap_{j=0}^{i-1}x(j)\notin D_f(j)\right][1-P_c(i-1)]\right\}\\
&\approx P[x(0)\in D_f(0)]\\
&\quad + \sum_{i=1}^{k}\{P[x(i)\in D_f(i)|x(i-1)\notin D_f(i-1)]\\
&\quad \times [1-P_c(i-1)]\}\\
&= P[x(t)\in D_f(t), \text{at least once in } [t_0,t_k]], \qquad \forall k>0
\end{aligned} \tag{17}$$

This provides an upper-bound approximation to $P_c(k)$ because

$$\begin{aligned}
&P[x(t)\in D_f(t), \text{at least once in } [t_0,t_k]]\\
&\quad \geq P[x(t)\in D_f(t), \text{exactly once in } [t_0,t_k]]
\end{aligned} \tag{18}$$

The approximation of Eq. (17) allows us to employ unconditional means to calculate Eq. (16), such that

$$f^{B(k)}_{\Gamma(k),\Delta\dot{\Gamma}(k)}(\gamma,\Delta\dot{\gamma}) = \frac{u(\gamma-\bar{\gamma})f_{\Gamma(k),\Delta\dot{\Gamma}(k)}(\gamma,\Delta\dot{\gamma})}{1-\int_{-\infty}^{+\infty}\int_{0}^{\bar{\gamma}} f_{\Gamma(k),\Delta\dot{\Gamma}(k)}(\gamma,\Delta\dot{\gamma})\,\mathrm{d}\gamma\,\mathrm{d}\Delta\dot{\gamma}} \tag{19}$$

where $u(\gamma-\bar{\gamma})$ is a unit step function and $f_{\Gamma(k),\Delta\dot{\Gamma}(k)}(\gamma,\Delta\dot{\gamma})$ is the joint PDF of $\gamma$ and $\Delta\dot{\gamma}$ at $t=t_k$, unconditional to conflict activity within $[t_0,t_k]$. The denominator is simply a scalar normalization according to Bayes rule.

The final approximation reduces the complexity of Eq. (15): Assume that $\gamma$ and $\Delta\dot{\gamma}$ are independent within any one time step $[t_k, t_{k+1}]$. The validity of this assumption is proven in Ref. 24, and errors resulting from it may be corrected to first order–second moment.[8,24] It is essential to note that this is very different from assuming that $\gamma$ and $\dot{\gamma}$ are independent within the entire $[t_0, t_{K-1}]$.

After the assumptions are combined and Leibniz's rule (see Ref. 25) is applied, rewrite Eq. (15) as

$$\begin{aligned}
f_{\Gamma(k+1)}(\gamma)|B[0,k] &\approx f_{\Gamma(k+1)}(\gamma)|B[k,k]\\
&= f^{B(k)}_{\Gamma(k)}(\gamma)\times f_{\Delta\dot{\Gamma}(k)}(\Delta\dot{\gamma})
\end{aligned} \tag{20}$$

where

$$f^{B(k)}_{\Gamma(k)}(\gamma) = \frac{u(\gamma-\bar{\gamma})f_{\Gamma(k)}(\gamma)}{1-\int_0^{\bar{\gamma}} f_{\Gamma(k)}(\gamma)\,\mathrm{d}\gamma} \tag{21}$$

and $f_{\Gamma(k)}(\gamma)$ and $f_{\Delta\dot{\Gamma}(k)}(\Delta\dot{\gamma})$ are the marginal PDFs of $\gamma$ and $\Delta\dot{\gamma}$, respectively, without conditioning on conflict events. The marginal PDFs may be found through mean and covariance propagation within a suitable state estimation filter, for example, an unscented Kalman filter. The usual Bayesian normalization factor is again present in the denominator.

It is Eq. (20), a one-dimensional convolution, combined with the ability to operate on the unconditional marginal PDFs of $\gamma$ and $\Delta\dot{\gamma}$ to find $P_c(k)$, that makes the solution to this problem tractable. It is shown in Sec. II.F.1 that the required marginal PDFs may be calculated for a quadratic representation of normally distributed state variables.

Figure 4 shows how to go about solving for $P_c(k)$ at each time step $t=t_k$. Figure 4 may be contrasted to the exact full-state calculation in Fig. 3.

When it is assumed that the unconditional marginal PDFs of $\gamma$ and $\Delta\dot{\gamma}$ are known, the process of finding $P_c(k)$ and propagating $f_{\Gamma(k+1)}(\gamma)|B[k,k]$ may be divided into the following steps.

1) Find $g_{A(k)}(\gamma)$, the segment of $f_{\Gamma(k)}(\gamma)|B[k-1,k-1]$ for which $\gamma \leq \bar{\gamma}$.

2) Make use of

$$P_c(k) = P_c(k-1) + \int_0^{\bar{\gamma}} g_{A(k)}(\gamma)\,\mathrm{d}x[1-P_c(k-1)]$$

to accumulate the probability of conflict.

3) Apply Eq. (21) to find $f^{B(k)}_{\Gamma(k)}(\gamma)$. Note that this step does not rely on steps 1 and 2.

4) Apply Eq. (20) to propagate $f^{B(k)}_{\Gamma(k)}(\gamma)$ into $f_{\Gamma(k+1)}(\gamma)|B[k,k]$.

Now continue by returning to step 1 for calculation of $P_c(k+1)$ and so forth.

A clear segmentation between the outlined steps is evident. This is because Eq. (17) allows us to express Eqs. (18) and (21) as functions of unconditional marginal PDFs that are independent of the conditional operations at the previous time $t=t_{k-1}$. The conditional PDF, $f_{\Gamma(k+1)}(\gamma)|B[k,k]$, in step 4 is created by assuming independence between $\gamma$ and $\Delta\dot{\gamma}$ within only one time step.

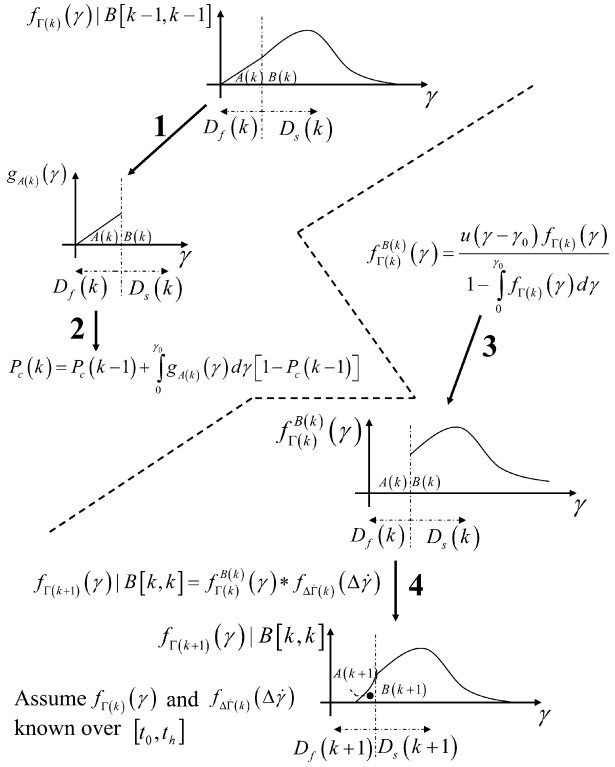


**Fig. 4 Four-step $f_{\Gamma(k+1)}(\gamma)|B[k,k]$ propagation and calculation of $P_c(k)$.**

An alternate view of the apparent segmentation is that the independence assumption is only employed over the course of one time step and only to determine the amount of flow of probability into $D_f(k)$. The seemingly simpler route of assuming independence within the entire interval $[t_0, t_h]$ and using it to propagate $f_{\Gamma(k+1)}(\gamma)|B[0,k]$ through the resulting simple one-dimensional convolution, is folly because convolution then always leads to an increase in the variance of the PDF. In reality, the variance of a quadratic metric should reduce drastically when its mean approaches $\bar{\gamma}$ because its chi-square distribution narrows when it nears the origin.

*1. Methods of Solution*

The focus now becomes finding a solution to $f_{\Gamma(k)}(\gamma)$ and $f_{\Delta\dot{\Gamma}(k)}(\Delta\dot{\gamma})$ within $[t_0, t_h]$. This paper only details how to solve for $f_{\Gamma(k)}(\gamma)$ and eventually proves that $f_{\Delta\dot{\Gamma}(k)}(\Delta\dot{\gamma})$ may be solved in a similar way.

The PDF of a general quadratic form of normally distributed random variables needs to be approximated. A number of special cases do exist, but are not discussed here.[24] Methods of approximation include series expansion, numerical Fourier inversion, Monte Carlo, and particle-based filtering simulations and approximations based on moment matching techniques. Moment matching through processes such as Cornish–Fisher, Gram–Charlier and Edgeworth expansion (see Refs. 26 and 27) do not provide accurate results when tails of PDFs are of value and provide little or no guarantee on rates of convergence relative to the number of cumulants matched.[26] In this case, Monte Carlo techniques are computationally expensive when exploring high-dimensional probability spaces, again, because of the high accuracy required when representing the tails of estimated PDFs, as with most problems in risk and reliability theory. It is partly for this reason that Yang[5] also performs a dimensional reduction to vehicle heading, before attempting Monte Carlo simulation.

Fourier inversion emerges as the salient choice because it turns out that the inversion process can be greatly simplified for the quadratic conflict metric. When applying Fourier inversion, one would first need to solve for the marginal characteristic function of $\gamma$ given by

$$\phi_{\Gamma(k)}(\tau) = E[e^{j\tau\gamma}] = \int_{-\infty}^{+\infty} e^{j\tau\gamma} f_\Gamma(\gamma)\,\mathrm{d}\gamma \tag{22}$$

and then solve for the Fourier inversion integral (FII)

$$f_{\Gamma(k)}(\gamma) = \frac{1}{2\pi}\int_{-\infty}^{+\infty} \phi_{\Gamma(k)}(\tau) e^{-jw\gamma}\,\mathrm{d}\tau \tag{23}$$

*2. Characteristic Function*

The next few paragraphs show that a closed-form solution to $\phi(\tau)$ does exist in an analytical form, when dealing with the proposed quadratic metric. First transform $\gamma$ into an appropriate form using the substitution $y = (x - m_X)$, where $m_X$ is the vector mean representation of $x$. In this way,

$$\begin{aligned}\gamma &= x^T B x \\ &= m_X^T B m_X + 2 m_X^T B y + y^T B y \\ &= \Theta + \Delta^T y + \tfrac{1}{2} y^T M y\end{aligned} \tag{24}$$

When solving the generalized eigenvalue problem such that

$$CC^T = \Sigma_X, \qquad C^T M C = \Lambda \tag{25}$$

where $\Lambda = \mathrm{diag}(\lambda_1, \ldots, \lambda_n)$, substitute $y = Cz$ and $\delta = C^T\Delta$ into Eq. (24) such that

$$\begin{aligned}\gamma &= \Theta + \delta^T z + \frac{1}{2} z^T \Lambda z \\ &= \Theta + \sum_{i=1}^{n}\left(\delta_i z_i + \frac{1}{2}\lambda_i z_i^2\right)\end{aligned} \tag{26}$$

where $z = (z_1, \ldots, z_n)^T$ is a standard normal vector and $\delta = (\delta_1, \ldots, \delta_n)^T \in \Re^n$. Now reshape $\phi_{\Gamma(k)}(\tau)$ into

$$\begin{aligned}\phi_{\Gamma(k)}(\tau) &= E[e^{j\tau\gamma}] \\ &= \int_{-\infty}^{+\infty} e^{j\tau\gamma} f_{\Gamma(k)}(\gamma)\,\mathrm{d}\gamma \\ &= e^{j\tau\Theta} E\left[e^{j\tau(\gamma-\Theta)}\right]\end{aligned} \tag{27}$$

and recognize that $E[e^{j\tau(\gamma-\Theta)}] = \phi_{\chi^2}(\tau)$, where $\phi_{\chi^2}(\tau)$ is the characteristic function of a noncentral chi-square ($\chi^2$) variate in $z$, where $z$ is in standard normal form. Here $\phi_{\chi^2}(\tau)$ is known analytically[26] and when substituted into Eq. (27) $\phi_{\Gamma(k)}(\tau)$ becomes

$$\phi_{\Gamma(k)}(\tau) = \exp(j\tau\Theta)\prod_{i=1}^{n}\frac{1}{\sqrt{1-j\lambda_i\tau}}\exp\left[\frac{-\frac{1}{2}\delta_i^2\tau^2}{(1-j\lambda_i\tau)}\right] \tag{28}$$

an analytical form to be substituted into Eq. (23), requiring no numerical approximation. The computational complexity of function evaluations in Eq. (28) is $\mathcal{O}(nN)$ and that of the eigenvalue decomposition [Eq. (25)] is in general $\mathcal{O}(n^3)$. The latter may be reduced to $\mathcal{O}(n^2)$.

*3. FII*

Various options exist when attempting to solve the inverse Fourier integral [Eq. (23)] using the characteristic function in Eq. (28). The most accepted method amounts to using fast Fourier transform (FFT) algorithms to reduce computational cost from $\mathcal{O}(N^2)$ to $\mathcal{O}[N\log_2(N)]$. As is the usual practice in engineering,[28] define the Fourier transform (FT) as

$$\mathcal{F}: f(x) \mapsto F(u) = \int_{-\infty}^{+\infty} e^{-j2\pi ux} f(x)\,\mathrm{d}x \tag{29}$$

Substituting $u = -t/2\pi$ into Eq. (29) results in

$$F(u) = \phi_{\Gamma(k)}(-2\pi u) \tag{30}$$

Now attempt to find $f(x) = f_{\Gamma(k)}(\gamma)$ by inverse FT (IFT), which is clearly equivalent to applying Eq. (23), the FII. All numerical solutions to IFT are approximate, unless $f(x)$ is continuous in $x$, periodic with period $T$, and band limited to frequencies $|u| < N/2T$, where the integer $N$ represents the number of discrete samples. One does not expect $f(x)$ to be periodic because, by definition,

$$\int_{-\infty}^{+\infty} f(x)\,\mathrm{d}x = 1$$

Hughett[29] shows that FFT approximation of $f(x)$ may now be accomplished by first splitting it into $f(x) = f_c(x) + \mathcal{C}$, where $f_c(x)$ is absolutely integrable and $\mathcal{C}$ is a constant. This split is done to avoid singularity problems when applying the FT.

Proakis and Manolakis[28] show how solution of the Fourier series through

$$f(x) \approx g(x) = \sum_{k=-N/2}^{N/2} G[k] \exp\left(\frac{j2\pi kx}{T}\right) \tag{31}$$

where $G[k]$ is defined by

$$G[k] = \begin{cases} F(0)/T + \mathcal{C}, & \text{for } k = 0 \\ F(k/T)/T, & \text{for } 0 < |k| < N/2 \\ 0 & \text{for } |k| = N/2 \end{cases} \tag{32}$$

provides an effective and accurate numerical approximation of $f(x)$. Notice that Eq. (31) is usually defined as the inverse discrete FT and that it may be solved using the Radix-2 inverse FFT (IFFT) algorithm, as long as $N$ can be written in the form $N = 2^E$ where $E$ is a positive integer. IFFTs are accomplished with at most $N/2 \log_2(N)$ multiplications and $N \log_2(N)$ additions, thereby reducing computational complexity to $\mathcal{O}[N \log_2(N)]$.

*4. Concerning $\Delta\dot{\gamma}$*

Earlier sections have shown that $f_{\Gamma(k)}(\gamma)$ can be calculated within $[t_0, t_h]$ because $\gamma$ can be converted into the required quadratic form. It turns out that $\Delta\dot{\gamma}(k)$ can also be expressed in this quadratic form as shown in the following derivation, where $B$ is symmetric:

$$\begin{aligned} \gamma &= x^T B x \\ \Delta\dot{\gamma} &= \Delta t \dot{x}^T B x + \Delta t x^T B \dot{x} \\ &= 2\Delta t x^T A^T B x + 2\Delta t u^T(k) B_u^T B x + 2\Delta t w^T(k) B_w^T B x \\ &\sim x^T N x + S x \end{aligned} \tag{33}$$

with $N = 2\Delta t A^T B$ and $S = 2\Delta t (u^T(k) B_u^T B + w^T(k) B_w^T B)$, and where $\Delta t$ is the time step, such that $\Delta t = t_{k+1} - t_k$.

Equation (33) would be in a quadratic form similar to Eqs. (12) and (26), but for the term $2\Delta t w^T(k) B_w^T B x$, which contains the random variable $w(k)$, white noise. This single term would make the dimensional and computational reduction discussed so far intractable again, unless one imposes the constraint that $B_w^T B = [0]$. This constraint simply implies that no states that form part of the calculation of $\gamma$ may be under direct noise excitation. Jones[24] shows how this constraint usually holds for Newtonian systems and may be ensured for other systems. One may, therefore, find $f_{\Delta\dot{\Gamma}(k)}(\Delta\dot{\gamma})$ at any point $t_k$ within the interval $[t_0, t_{K-1}]$ from the PDF of $x$ calculated through mean and covariance propagation within an optimal estimator. This is done in the same way as outlined for $f_{\Gamma(k)}(\gamma)$ in the preceding sections.

Last, Sec. II.D requires that $\Delta\dot{\gamma}$ be written exactly in the complete square form described by Eq. (12) when calculating the covariance between $\gamma$ and $\Delta\dot{\gamma}$ in Eq. (40). It is not immediately obvious that one may always write $\Delta\dot{\gamma}$ as a complete square. It can, however, be shown that $\Delta\dot{\gamma}$ may be written in the complete square quadratic form whenever the only nonzero elements in $B$ are on its diagonal and all of the derivatives of states operated on by nonzero entries in $B$ are themselves inside the state vector.[24]

*5. Concerning Convolution*

Even though Eq. (20) only requires one-dimensional convolution, this still results in $\mathcal{O}(N^2)$ computational complexity. Convolution can, however, be accomplished by computing the characteristic functions of each of $\gamma(k)$ and $\Delta\dot{\gamma}(k)$ and multiplying these (not convolving) before applying the FII.[25] Earlier $\phi_{\Delta\dot{\Gamma}(k)}(\tau)$ is determined analytically by Eq. (28) and would require no additional computation; however, $f^B_{\Gamma(k)}(\gamma)$ needs to be calculated within $[t_0, t_{K-1}]$ by applying Eq. (21) at each time step. It can be shown that $\phi^B_{\Gamma(k)}(\tau)$ [the characteristic function of $f^B_{\Gamma(k)}(\gamma)$] may be determined in a similar way to that described when computing $f_{\Gamma(k)}(\gamma)$, but with an FFT algorithm.[29] The numerical complexity, thus, again reduces to $\mathcal{O}[N \log_2(N)]$.

## III. Calculation Issues and Errors

One may differentiate among two types of significant errors when calculating $P_c(k)$. The first is approximation error, in which simplifying assumptions lead us to calculate an approximate FPT solution. The second induced error is that of numerical calculation,[24] in which one solves for the approximate solution to a specific accuracy. Only approximation error is discussed because it is specifically related to the proposed solution algorithm. A number of additional and relatively insignificant error sources are discussed elsewhere.[24]

Approximation error may be further subdivided into two major attributing factors: first, finding an upper-bound approximation to $P_c(k)$ [Eq. (18)] and second, assuming a measure of independence between $\gamma(k)$ and $\Delta\dot{\gamma}(k)$ when performing the necessary calculations [Eq. (20)], so the upper bound is itself calculated with an amount of error. One calculates a signed calculation error because of the independence assumption, to narrow the envelope of error and more closely approximate the true value of $P_c(k)$.

### A. Upper-Bound Probability Error

In Sec. II.F, why the calculated $P_c(k)$ is an upper bound, that is, $P_c(k) \equiv P_c^{\text{ub}}(k)$, to the true value denoted by $P_c^{\text{true}}(k)$, with ub signifying upper bound is described. It is infeasible to attempt to solve directly for the amount of error between the calculation and the true value because the true value would need to be derived from an intractable calculation. Define the error as

$$P_c^{\text{ube}}(k) = P_c^{\text{ub}}(k) - P_c^{\text{true}}(k) = P_c(k) - P_c^{\text{true}}(k) \tag{34}$$

with ube signifying the upper bound error. Define a lower bound to $P_c^{\text{true}}(k)$, denoted by $P_c^{\text{lb}}(k) \le P_c^{\text{true}}(k)$. Now use the lower bound to rewrite Eq. (34) as

$$P_c^{\text{ube}}(k) \le P_c(k) - P_c^{\text{lb}}(k) \tag{35}$$

A feasible lower bound would allow us to clamp the true probability of conflict between two calculable limits. One such intuitive and simple lower bound often used in estimation theory and also employed by Prandini et al.[30] to calculate probability of conflict is given by

$$P_c^{\text{lb}}(k) = \max \int_0^{\tilde{\gamma}} f_{\Gamma(\zeta)}(\gamma)\,\mathrm{d}\gamma, \qquad 0 \le \zeta \le k \tag{36}$$

This calculates the largest probability of state space intersecting with $D_f(t)$ within a period of time. Various texts,[31,32] especially in the field of satellite conflict avoidance, exist where Eq. (36) is used to approximate $P_c^{\text{true}}(k)$. This is, however, a dangerous course of action for general aeronautical applications because there is no guarantee on the lower bound's error, potentially compromising on safety. Equation (36) is so simple, however, that it only adds complexity of $\mathcal{O}(nN)$ to the calculations performed at each time step. That being said, the equation makes for a useful lower bound, rather than an estimate of $P_c^{\text{true}}(k)$.

### B. Calculation Error

Independence between $\gamma$ and $\Delta\dot{\gamma}$ is equivalent to a combination of two assumptions.

1) It is assumed that $f^{B(k)}_{\Delta\dot{\Gamma}(k)}(\Delta\dot{\gamma}) = f_{\Delta\dot{\Gamma}(k)}(\Delta\dot{\gamma})$, thereby implying that the segmentation of probability space inside and outside of $D_f(t)$ and the subsequent creation of $f^{B(k)}_{\Gamma(k)}(\gamma)$ has no effect on the conditional distribution of $\Delta\dot{\gamma}$.

2) Convolution may be employed to express

$$f_{\Gamma(k+1)}(\gamma)|B[k,k] = f^{B(k)}_{\Gamma(k)}(\gamma) \times f_{\Delta\dot{\Gamma}(k)}(\Delta\dot{\gamma})|B[0,k-1] \quad (37)$$

where Eq. (15) is the combination of items 1 and 2.

The two enumerations will be referred to as assumptions 1 and 2, respectively. Before continuing, one needs to acquire a number of mathematical tools describing the relationship between $\gamma$ and $\Delta\dot{\gamma}$ to characterize error.

Describe the expected value of a quadratic form $x^T B\boldsymbol{x}$ of the multivariate normally distributed random vector $\boldsymbol{x}$ as

$$\boldsymbol{E}(x^T B\boldsymbol{x}) = \mathrm{tr}(B\Sigma_x) + \mu_x^T B\mu_x \quad (38)$$

where $\Sigma_x$ and $\mu_x$ are the covariance matrix and mean vector of $\boldsymbol{x}$ respectively. The variance becomes

$$\sigma^2_{x^T Bx} = \mathrm{var}(x^T B\boldsymbol{x}) = 2\mathrm{tr}(B\Sigma_x B\Sigma_x) + 4\mu_x^T B\Sigma_x B\mu_x \quad (39)$$

and the covariance between two quadratic forms $y_1 = x^T B\boldsymbol{x}$ and $y_2 = x^T P\boldsymbol{x}$ can be described by

$$\rho\sigma_{y1}\sigma_{y2} = \mathrm{cov}(x^T B\boldsymbol{x}, x^T P\boldsymbol{x}) = 2\mathrm{tr}(B\Sigma_x P\Sigma_x) + 4\mu_x^T B\Sigma_x P\mu_x \quad (40)$$

From these equations, construct the mean vector of the joint density for $h = [y_1, y_2]^T$ as

$$\boldsymbol{E}[h] = [m_{y_1}, m_{y_1}]^T \quad (41)$$

and the covariance matrix

$$\Sigma_h = \begin{bmatrix} \sigma^2_{y_1} & \rho\sigma_{y_1}\sigma_{y_2} \\ \rho\sigma_{y_1}\sigma_{y_2} & \sigma^2_{y_2} \end{bmatrix} \quad (42)$$

The next step is to be able to describe the orthogonal principal axes of the symmetric matrix $\Sigma_h$. This is done through eigenvector decomposition, and after some algebra the slope of the principal axis with the same sign as $\rho$ is given by

$$m = \frac{\left[-\sigma^2_{y_2} + \sigma^2_{y_1} + \left(\sigma^4_{y_2} - 2\sigma^2_{y_1}\sigma^2_{y_2} + \sigma^4_{y_1} + 4\rho^2\sigma^2_{y_1}\sigma^2_{y_2}\right)^{\frac{1}{2}}\right]}{2\rho\sigma_{y_1}\sigma_{y_2}} \quad (43)$$

such that the correlation line $y_1 = my_2 + c$ is created. If $\gamma = y_1$ and $\Delta\dot{\gamma} = y_2$, then Fig. 5 provides additional clarity with a contour plot of the joint density function $f_{\Gamma,\Delta\dot{\Gamma}}(\gamma, \Delta\dot{\gamma})$. Next describe the first-order–second-moment (FOSM) change in $f_{\Delta\dot{\Gamma}(k)}(\Delta\dot{\gamma})$ because of an FOSM change in $f_{\Gamma(k)}(\gamma)$. This is the characterization of error because of assumption 1.

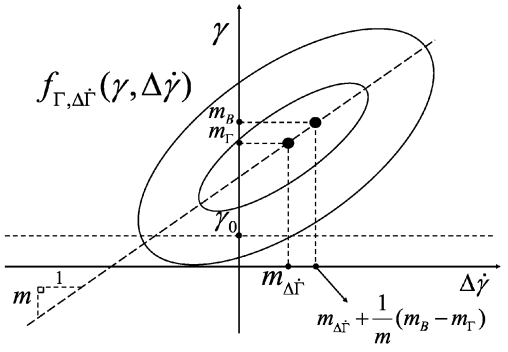


**Fig. 5 Contours of $f_{\Gamma,\dot{\Gamma}}(\gamma,\dot{\gamma})$ with correlation line.**

Here, $f_{\Gamma(k)}(\gamma)$ and $f_{\Delta\dot{\Gamma}(k)}(\Delta\dot{\gamma})$ comprise well-behaved summed and scaled versions of noncentral chi-square distributions. The maximum allowable $P_c(k)$ within $[t_0, t_h]$, denoted by $P_{c_{\max}}$, is a very small number (typically $P_{c_{\max}} < 0.05$). Furthermore, make the reasonable assumption to take action along any flight path such that $P_c(k) < P_{c_{\max}}$ always holds. With use of these assumptions, calculate the expected influence on the mean and variance of $f^{B(k)}_{\Delta\dot{\Gamma}(k)}(\Delta\dot{\gamma})$ because of adjustments to $f_{\Gamma(k)}(\gamma)$, such as the removal of $\Delta P_c(k)$ probability space to form $f^{B(k)}_{\Gamma(k)}(\gamma)$. When

$$\Delta P_c(k) = \int_0^{\bar{\gamma}} f_{\Gamma(k)}(\gamma)\,\mathrm{d}\gamma \quad (44)$$

is defined, then, as before, the PDF of $\gamma$ is split into

$$\begin{aligned} f_{\Gamma(k)}(\gamma) &= g_{A(k)}(\gamma) + g_{B(k)}(\gamma) \\ &= \Delta P_c(k) f^{A(k)}_{\Gamma(k)}(\gamma) + [1 - \Delta P_c(k)] f^{B(k)}_{\Gamma(k)}(\gamma) \end{aligned} \quad (45)$$

Here the mean and variance of, for example, $f^{A(k)}_{\Gamma}(\gamma)$ are denoted by $m_{A(k)}$ and $\sigma^2_{A(k)}$ respectively. Now focus on the expected value of $\gamma$ after the removal of probability space within $D_f(k)$, that is, given that $\gamma > \bar{\gamma}$. This is expressed as

$$\boldsymbol{E}[\gamma]|(\gamma > \bar{\gamma}) \equiv m_{B(k)} = \boldsymbol{E}[\gamma(k)] + \Delta\boldsymbol{E}[\gamma(k)] \quad (46)$$

where $\Delta\boldsymbol{E}[\gamma(k)]$ is the change in the mean of $\gamma$ after the cut. Notice that $m_{B(k)} \geq \boldsymbol{E}[\gamma(k)]$ and, therefore, $\Delta\boldsymbol{E}[\gamma(k)] \geq 0$.

Equation (46) can be rewritten as

$$\begin{aligned} \Delta\boldsymbol{E}[\gamma(k)] &= m_{A(k)} - \boldsymbol{E}[\gamma(k)] \\ &= \{\Delta P_c(k)/[1 - \Delta P_c(k)]\}\left\{\boldsymbol{E}[\gamma(k)] - m_{A(k)}\right\} \\ &= \{\Delta P_c(k)/[1 - \Delta P_c(k)]\}\left(m_{\Gamma(k)} - m_{A(k)}\right) = \Delta m_{\Gamma(k)} \end{aligned} \quad (47)$$

with $m_{A(k)} \equiv \boldsymbol{E}[\gamma]|(0 \leq \gamma < \bar{\gamma})$. Thus, if the mean of $\gamma$ changes by $\Delta\boldsymbol{E}[\gamma(k)]$, then one may employ Eq. (43) to show that the mean of $\Delta\dot{\gamma}$ changes by $(1/m)\Delta\boldsymbol{E}[\gamma(k)]$. With $\boldsymbol{E}[\Delta\dot{\gamma}_k^{B_k}] = \boldsymbol{E}[\Delta\dot{\gamma}_k] + \Delta\boldsymbol{E}[\Delta\dot{\gamma}_k]$, then express

$$\begin{aligned} \Delta m_{\Delta\dot{\Gamma}(k)} &\equiv \Delta\boldsymbol{E}[\Delta\dot{\gamma}(k)] \\ &= \frac{2\rho\sigma_\Gamma\sigma_{\Delta\dot{\Gamma}}}{\left[-\sigma^2_{\Delta\dot{\Gamma}} + \sigma^2_\Gamma + \left(\sigma^4_{\Delta\dot{\Gamma}} - 2\sigma^2_\Gamma\sigma^2_{\Delta\dot{\Gamma}} + \sigma^4_\Gamma + 4\rho^2\sigma^2_\Gamma\sigma^2_{\Delta\dot{\Gamma}}\right)^{\frac{1}{2}}\right]} \\ &\quad \times \frac{\Delta P_c(k)}{1 - \Delta P_c(k)}\left(m_{\Gamma(k)} - m_{A(k)}\right) \end{aligned} \quad (48)$$

The change in variance $(\Delta\sigma^2_{\Gamma(k)})$ may described in a similar way such that

$$\begin{aligned} \Delta\sigma^2_{\Gamma(k)} &= \sigma^2_{B(k)} - \sigma^2_{\Gamma(k)} \\ &= \frac{1}{1 - \Delta P_c(k)}\left\{\sigma^2_{\Gamma(k)} - 2\frac{\Delta P_c(k) m_{\Gamma(k)}}{1 - \Delta P_c(k)} m_{\Gamma(k)} \right. \\ &\quad \left. + \left[\frac{m - \Delta P_c(k) m_{A(k)}}{1 - \Delta P_c(k)}\right]^2 - m^2_{\Gamma(k)}\right\} \\ &\quad - \frac{\Delta P_c(k)}{1 - \Delta P_c(k)}\left\{\sigma^2_{A(k)} - 2\frac{m_{\Gamma(k)} - m_{A(k)}}{1 - \Delta P_c(k)} m_{A(k)} \right. \\ &\quad \left. + \left[\frac{m - \Delta P_c(k) m_{A(k)}}{1 - \Delta P_c(k)}\right]^2 - m^2_{A(k)}\right\} - \sigma^2_{\Gamma(k)} \end{aligned} \quad (49)$$

The change in the variance of $\dot{\gamma}$ is given by

$$\Delta\sigma^2_{\Delta\dot{\Gamma}(k)} = (1/m)^2\Delta\sigma^2_{\Gamma(k)} \tag{50}$$

Equations (48) and (50) are representations of the changes in mean and variance of $\Delta\dot{\gamma}$, given the first-order approximation that the mapping of the first two moments from $\gamma$ to $\Delta\dot{\gamma}$ may be accomplished through the correlation line with slope $m$. This approximation is only feasible for small values of $\Delta P_c(k)$ associated with small time steps of calculation $\Delta t$.

Next we return to assumption 2 and form the combined FOSM error estimates because of assumptions 1 and 2. Recall that the assumption 2 error is induced by determining the probability density of

$$\gamma(k+1) = \gamma(k) + \Delta\dot{\gamma}(k) \tag{51}$$

through convolution of the conditional marginal PDF of $\gamma(k)$ and the unconditional marginal PDF $\Delta\dot{\gamma}(k)$ instead of operating on the joint density. Elementary statistics dictate that the true mean and variance of $\gamma(k+1)$ be described by

$$m^{\text{true}}_{\Gamma(k+1)} = m^{\text{true}}_{\Gamma(k)} + m^{\text{true}}_{\Delta\dot{\Gamma}(k)} \tag{52}$$

$$\sigma^{2\cdot\text{true}}_{\Gamma(k+1)} = \sigma^{2\cdot\text{true}}_{\Gamma(k)} + \sigma^{2\cdot\text{true}}_{\Delta\dot{\Gamma}(k)} - 2\rho(k)\sigma^{\text{true}}_{\Gamma(k)}\sigma^{\text{true}}_{\Delta\dot{\Gamma}(k)} \tag{53}$$

respectively. The convolution process maintains Eq. (52), so that the only error in the mean results from assumption 1. Therefore, the error on $m_{\Gamma(k+1)}$ accumulated within the single time step $[t_k, t_{k+1}]$ can be written as $\nabla m_{\Gamma(k+1)} \equiv \Delta m_{\Delta\dot{\Gamma}(k)}$, which is the direct application of Eq. (47) such that

$$\begin{aligned} m^{\text{ub}}_{\Gamma(k+1)} &\approx m^{\text{FOSM}}_{\Gamma(k+1)} \\ &= m^{\text{calculated}}_{\Gamma(k+1)} + \nabla m_{\Gamma(k+1)} \end{aligned} \tag{54}$$

The induced variance error over the same time step is described in a similar way, becoming

$$\nabla\sigma^2_{\Gamma(k+1)} \equiv \Delta\sigma^2_{\Delta\dot{\Gamma}(k)} - 2\rho(k)\sigma_{\Gamma(k)}\left(\sigma_{\Delta\dot{\Gamma}(k)} + \Delta\sigma_{\Delta\dot{\Gamma}(k)}\right) \tag{55}$$

with the first term originating from Eq. (50). The second term, in keeping with FOSM approximation, is provided by Eq. (40) because of assumption 2. In this case,

$$\begin{aligned} \sigma^{2\cdot\text{ub}}_{\Gamma(k+1)} &\approx \sigma^{2\cdot\text{FOSM}}_{\Gamma(k+1)} \\ &= \sigma^{2\cdot\text{calculated}}_{\Gamma(k+1)} + \nabla\sigma^2_{\Gamma(k+1)} \end{aligned} \tag{56}$$

In the spirit of FOSM analysis, an FOSM matching may be performed between $f^{\text{ub}}_{\Gamma(k+1)}(\gamma)|B[k,k] \approx f^{\text{FOSM}}_{\Gamma(k+1)}(\gamma)|B[k,k]$ and $f^{\text{calculated}}_{\Gamma(k+1)}(\gamma)|B[k,k]$ to provide a more accurate calculation of $f^{\text{ub}}_{\Gamma(k+1)}(\gamma)|B[k,k]$. Jones[24] derives a very simple implementation of this FOSM correction, with minimal impact on the solution algorithm for $P_c(k)$, as an equivalent adjustment to the DMOD ($\bar{\gamma}$) at each time step, to become

$$\bar{\gamma}_{\text{Adj}} \equiv \frac{\sqrt{\sigma^{2\cdot\text{calculated}}_{\Gamma(k)} + \nabla\sigma^2_{\Gamma(k+1)}}}{\sigma^{\text{calculated}}_{\Gamma(k+1)}}\bar{\gamma} - \nabla m_{\Gamma(k+1)} \tag{57}$$

Note that such a FOSM corrected calculation may be always be utilized as a corrected measure of $P_c(k)$, but then higher-order moments need to be determined if one is interested in characterizing the remaining error.

## IV. Example Application

### A. Vehicle Description

The New Generation Mini-II (NGM-II)[33] is an autonomous UAV developed by the Massachusetts Institute of Technology (MIT) under the MIT/Draper Technology Development Partnership Program. The vehicle is operated at medium and low altitudes where obstacles such as trees (or tree trunks), buildings, communication towers and the like are abundant.

The NGM-II is an 8-kg, fixed-wing, single-engine aircraft with a pusher configuration, a wing span of approximately 2 m and length of 1.5 m. Its dynamics may be likened to a large sport or aerobatic model remote control aircraft.

A simplified two-dimensional, linear time-invariant, closed-loop dynamic model of the aircraft, under free-flight conditions, was created with the assistance of the main architect of its control system.[34]

The conflict scenario simulates the NGM-II flying past a stationary, tree trunk-sized hazard in close proximity, while commanded to hold a straight-line trajectory with a forward airspeed of 20 m/s, in a wind-free environment. The proximity with which it passes the obstacle is representative of the maximum acceptable conflict risk allowed for this vehicle, chosen to be $P^{\max}_c = 0.05$. The resulting $P_c(t_h)$ will, therefore, be representative of a level of risk when conflict avoidance action will typically be taken.

A mean (hazard) passage time (MPT) is provided, and is denoted by $\bar{t}_{\text{MPT}}$. The MPT indicates when a vehicle passed the center of the domain of failure. More, precisely, for the straight-line flight paths here, $\bar{t}_{\text{MPT}}$ is the only time when the mean of $\dot{\Gamma}$ is zero, that is, it is changing sign. In this instance, $\bar{t}_{\text{MPT}} = 1.09$ s.

### B. Simulation Results

Figure 6 shows the results of accumulation of risk within a time window $t = [t_1, t_2]$, where $t_0 < t_1 < t_2 < t_h$, within a certain finite horizon time window. The four distinct curves in Fig. 6 are related to each other as follows.

The solid line represents a close approximation of the true probability of conflict $[P^{\text{true}}_c(t)]$ up to time $t = t_h$, obtained from a high-fidelity Monte Carlo simulation with negligible [1% of $P(t)$] error. This is denoted by $P^{\text{true}}_c(t)$. The algorithms for calculation of conflict risk, developed herein, are represented by curves of $P_c(t)$ and $P^{\text{FOSM}}_c(t)$. A lower bound probability of conflict, $P^{\text{lb}}_c(t_h)$, is determined, as described by Eq. (36).

Figure 6 shows how $P_c(t)$ and $P^{\text{FOSM}}_c(t)$ are accumulated over a shorttime window, as the vehicle passes the hazard, again emphasizing the similarities between conflict probability and the FPT problem discussed in Sec. I.C. Figure 6 shows the upper-bounded nature of $P_c(t_h)$ because it is larger than $P^{\text{true}}_c(t_h)$ and also shows the lower-bounded nature of $P^{\text{lb}}_c(t)$, which is clearly smaller than $P^{\text{true}}_c(t)$.

$P^{\text{FOSM}}_c(t_h)$ is within 8% of $P^{\text{true}}_c(t_h)$, and $P_c(t_h)$ is within 6% of $P^{\text{true}}_c(t_h)$. The seemingly more accurate $P_c(t)$ is not evidence of failure of the FOSM error correction method. $P_c(t)$ is an approximation of the upper bound of the probability of conflict, denoted by $P^{\text{ub}}_c(t)$, and $P^{\text{FOSM}}_c(t_h)$ is a more exact approximate of this $P^{\text{ub}}_c(t)$. It is circumstantial that $P_c(t_h) < P^{\text{FOSM}}_c(t_h)$, and it can be shown that the opposite inequality holds under different simulation conditions.[24]

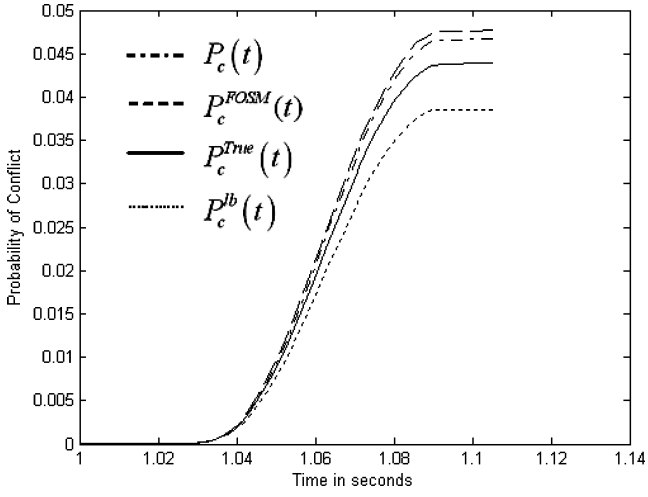


**Fig. 6 Risk accumulation for NGM-II flying past a hazard.**

**Table 1 Respective computation times for $t_h = 1.1$ s**

| Legend | Calculation method | Computation time, s |
|---|---|---|
| $P_c(t)$ | Non-FOSM corrected risk[24] | 4 |
| $P_c^{\text{FOSM}}(t)$ | FOSM corrected risk[24] | 5 |
| $P_c^{\text{true}}(t)$ | Pure Monte Carlo | 6450 |
| $P_c^{\text{lb}}(t)$ | Lower bound to risk[30] | 0.2 |

The independence assumption labeled assumption 1 in Sec. II.F. accounts for the approximately 2% difference between $P_c^{\text{FOSM}}(t_h)$ and $P_c(t_h)$.

$P_{c_h}^{\text{lb}}(t)$ is of special interest in Fig. 6 because it is approximately 15% smaller than $P_c^{\text{true}}(t_h)$. Using the lower bound alone to obtain an estimate of $P_c^{\text{true}}(t_h)$ would be much simpler to accomplish than the algorithm presented to find $P_c(t_h)$. The danger involved in trusting a lower bound of conflict risk would, however, make this a potentially catastrophic venture. $P_c^{\text{lb}}(t_h)$ and $P_c(t_h)$ do, however, bound $P_c^{\text{true}}(t_h)$.

Note that $P_c^{\text{lb}}(t_h)$ quickly becomes a progressively worse measure of $P_c^{\text{true}}(t_h)$, the more time is spent in the vicinity of $D_f$. One such example is when attempting to orbit a circular $D_f$ at a constant radius. $P_c^{\text{lb}}(t)$ will not grow as time progresses, whereas both $P_c^{\text{true}}(t_h)$ and $P_c(t_h)$ would increase.

The 1.1-s simulation was run in MATLAB® 6.1, on a 1-GHz Pentium 3-equivalent desktop computer running Windows NT 4.0. Table 1 lists the computation times for each trace in Fig. 6. Quadratic-space risk accumulation was accomplished at fixed 5-ms time steps.

Jones[24] details three additional simulation examples showing similar results, including a generic large commercial transport engaged in head-on and fly-by conflicts.

## V. Conclusions

Quadratic-order reductive conflict metrics are applied and provide a tractable and approximate solution to the general and intractable FPT problem of multidimensional conflict risk calculation within a finite time horizon. A tractable real-time algorithm is developed for the calculation of an accurate upper bound to conflict risk, as a function of time, along a deterministic flight trajectory. Such a proven upper bound is essential when designing safe systems. Calculation and approximation errors resulting from application of the algorithm are characterized and quantified. Simulations verify the accuracy of the conflict risk algorithm and the derived primary calculation error components.

## Acknowledgments

This research was conducted at the Massachusetts Institute of Technology (MIT)'s Department of Aeronautics and Astronautics. It was funded by the C. S. Draper Laboratory under the MIT/Draper Technology Development Partnership Program. Special thanks are extended to John J. Deyst Jr., James K. Kuchar, Lee Yang, Brent Appleby, Lorraine Fesq, Emilio Frazzoli, Sanghyuk Park, and Danielle Veneziano.

## References

[1]Kuchar, J. K., and Yang, L. C., "Survey of Conflict Detection and Resolution Modelling Methods," AIAA Paper 97-3732, Aug. 1997.

[2]Yang, L. C., and Kuchar, J. K., "Prototype Conflict Alerting Logic for Free Flight," *Journal of Guidance, Control, and Dynamics*, Vol. 20, No. 4, 1997, pp. 768–773.

[3]Kuchar, J. K., "A Unified Methodology for the Evaluation of Hazard Alerting Systems," Ph.D. Dissertation, Dept. of Aeronautics and Astronautics, Massachusetts Inst. of Technology, Cambridge, MA, 1995.

[4]Wickens, C., and Hollands, J., *Engineering Psychology and Human Performance*, 3rd ed., Prentice–Hall, Upper Saddle River, NJ, 1999, pp. 293–336.

[5]Yang, L. C., "Aircraft Conflict Analysis and Real-Time Conflict Probing Using Probabilistic Trajectory Modeling," Ph.D. Dissertation, Dept. of Aeronautics and Astronautics, Massachusetts Inst. of Technology, Cambridge, MA, 2000.

[6]Desilles, G., "Differential Kolmogorov Equations for Transiting Processes," M.S. Thesis, Dept. of Aeronautics and Astronautics, Massachusetts Inst. of Technology, Cambridge, MA, June 1998.

[7]Kuchar, J. K., "Methodology for Alerting-System Performance Evaluation," *Journal of Guidance, Navigation, and Dynamics*, Vol. 19, No. 2, 1996, pp. 438–444.

[8]Ang, A. H.-S., and Tang, W. H., *Probability Concepts in Engineering Planning and Design, Basic Principles*, Vol. 1, Wiley, New York, 1975, Chap. 9.

[9]Andrews, J. W., "A Relative Motion Analysis of Horizontal Collision," *SAFE Journal*, Vol. 8, No. 2, 1978, pp. 7, 8.

[10]Eby, M. S., "A Self-Organizational Approach for Resolving Air Traffic Conflicts," *Lincoln Laboratory Journal*, Vol. 7, No. 2, 1994, p. 239.

[11]Shewchun, M., Oh, J.-H., and Feron, E., "Linear Matrix Inequalities for Analysis of Free Flight Conflict Problems," *IEEE Conference on Decision and Control*, Vol. 3, Dec. 1997, pp. 2417–2422.

[12]Ford, R. L., and Powell, D. L., "A New Threat Detection Criterion for Airborne Collision Avoidance Systems," *Journal of Navigation*, Vol. 43, No. 3, 1990, pp. 391–403.

[13]Teo, R., and Tomlin, C., "Computing Danger Zones for Provably Safe Closely Spaced Parallel Approaches," *Journal of Guidance, Control, and Dynamics*, Vol. 26, No. 3, 2003, pp. 434–443.

[14]Patera, R. P., "Satellite Collision Probability for Nonlinear Relative Motion," *Journal of Guidance, Control, and Dynamics*, Vol. 26, No. 5, 2003, pp. 728–733.

[15]Yang, L. C., Yang, J. H., Kuchar, J. K., and Feron, E., "A Real-Time Monte Carlo Implementation for Computing Probability of Conflict," AIAA Paper 2004-4876, Aug. 2004.

[16]Borodin, A. N., and Salminen, P., *Handbook of Brownian Motion: Facts and Formulae*, 2nd ed., Birkhauser Verlag, Boston, 2002, Chap. 2.

[17]Gardiner, C. W., *Handbook of Stochastic Methods for Physics, Chemistry, and the Natural Sciences*, 2nd ed., Vol. 13, Springer Series in Synergetics, Springer-Verlag, New York, 1985, Chap. 4.

[18]Paielli, R. A., and Erzberger, H., "Conflict Probability Estimation for Free Flight," *Journal of Guidance, Control, and Dynamics*, Vol. 20, No. 3, 1997, pp. 588–596.

[19]Williamson, T., and Spencer, N. A., "Development and Operation of the Traffic Alert and Collision Avoidance System," *Proceedings of the IEEE*, Vol. 77, No. 11, 1989, pp. 1735–1744.

[20]"Minimum Performance Specifications for TCAS Airborne Equipment," Radio Technical Committee on Aeronautics (RTCA), Rept. RTCA/DO-185, Washington, DC, Sept. 1983.

[21]Veneziano, D., "Crossings and Extremes of Random Functions," Universita' di Firenze, Ingegneria Strutturale, Rept. UFIST/05/1979, Florence, Italy, June 1979.

[22]Shinozuka, M., and Yao, J. T. P., "On the Two-Sided Time-Dependent Barrier Problem," *Journal of Sound and Vibration*, Vol. 6, No. 1, 1967, pp. 98–104.

[23]Crandall, S. H., "First-Crossing Probabilities of the Linear Oscillator," *Journal of Sound and Vibration*, Vol. 12, No. 3, 1970, pp. 285–299.

[24]Jones, T., "Real-Time Probabilistic Collision Avoidance for Autonomous Vehicles, Using Order Reductive Conflict Metrics," Ph.D. Dissertation, Dept. of Aeronautics and Astronautics, Massachusetts Inst. of Technology, Cambridge, MA, June 2003.

[25]Peebles, P. Z., Jr., *Probability, Random Variables, and Random Signal Principles*, 3rd ed., McGraw–Hill, Singapore, 1993, pp. 115–118.

[26]Jaschke, S., "The Cornish–Fisher–Expansion in the Context of Delta–Gamma–Normal Approximations," *Journal of Risk*, Vol. 4, No. 4, 2002, pp. 33–52.

[27]Barndorff-Nielsen, O., and Kluppelberg, C., "Tail Exactness of Multivariate Saddlepoint Approximations," *Scandinavian Journal of Statistics*, Vol. 26, No. 2, 1999, pp. 253–264.

[28]Proakis, J. G., and Manolakis, D. G., *Digital Signal Processing: Principles, Algorithms, and Applications*, 3rd ed., Prentice–Hall, Upper Saddle River, NJ, 1996, pp. 230–393.

[29]Hughett, P., "Error Bounds for Numerical Inversion of a Probability Characteristic Function," *SIAM Journal on Numerical Analysis*, Vol. 35, No. 4, 1998, pp. 1368–1392.

[30]Prandini, M., Hu, J., Lygeros, J., and Sastry, S., "A Probabilistic Approach to Aircraft Conflict Detection," *IEEE Transactions on Intelligent Transportation Systems*, Vol. 1, No. 4, 2000, pp. 199–220.

[31]Chan, F. K., "Collision Probability Analysis for Earth-Orbiting Satellites," Inst. of Electrical and Electronics Engineers, *Core Technologies for Space Systems Conference*, Nov. 2001.

[32]Akella, M. R., and Alfriend, K. T., "Probability of Collision Between Space Objects," *Journal of Guidance, Control, and Dynamics*, Vol. 23, No. 5, 2000, pp. 769–772.

[33]Jones, T., and Jourdan, D., "The Parent and Child Unmanned Aerial Vehicle System," Association for Unmanned Vehicle Systems International (AUVSI) Symposium, July 2003.

[34]Park, S., "Avionics and Control System Development for Mid-Air Rendezvous of Two Unmanned Aerial Vehicles," Ph.D. Dissertation, Dept. of Aeronautics and Astronautics, Massachusetts Inst. of Technology, Cambridge, MA, Feb. 2004.